Curr Genet (2006) 49: 351–363
DOI 10.1007/s00294-006-0061-6

RESEARCH ARTICLE

Monica A. Schwartz · Hiten D. Madhani

Control of MAPK signaling specificity by a conserved residue in the MEK-binding domain of the yeast scaffold protein Ste5

Received: 9 January 2006 / Revised: 17 January 2006 / Accepted: 18 January 2006 / Published online: 4 February 2006

Abstract The yeast kinase scaffold Ste5 has been proposed to prevent unwanted cross-talk between the pheromone response pathway and other MAPK cascades. Protein fusion experiments have demonstrated that covalently tethering signaling components to each other or to Ste5 can determine the outcome of signaling. However, these do not fully test the role of scaffolds in signaling specificity, since fusing components precludes differential dissociation of subpopulations. We performed a targeted genetic screen on *STE5* and repeatedly identified recessive mutations in a conserved residue, E756, in the Ste7/MEK-binding domain that caused erroneous activation of the filamentation MAPK pathway by pheromone signaling. Mutant cells exhibited a shift in the MAPK activation pattern such that the filamentation MAPK Kss1 was predominately activated in response to pheromone. Velocity sedimentation studies showed that the mutant scaffold was defective in binding to a phosphorylated subpopulation of Ste7. Our data suggest that increased dissociation of activated Ste7 kinase from the mutant scaffold may cause the observed shift in MAPK activation from Fus3 to Kss1 and the resulting loss of specificity. Cross-talk in *ste5-E756G* cells was due to both increased activation of Kss1 and reduced Fus3-dependent degradation of the filamentation pathway transcription factor Tec1. These studies demonstrate a role for an endogenous scaffold in signaling specificity.

Keywords Ste5 · Ste7 · Scaffold · Specificity · Activated kinase

Communicated by S. Hohmann

M. A. Schwartz · H. D. Madhani (✉)
Department of Biochemistry and Biophysics,
University of California, San Francisco, 600 16th St,
San Francisco, CA 94143-2200, USA
E-mail: hiten@biochem.ucsf.edu
Tel.: +1-415-5140594
Fax: +1-415-5024315

Introduction

A central question in cell biology concerns how signal transduction systems that share components maintain specificity. Such pathways are activated by different extracellular signals and lead to distinct intracellular responses, yet the signals are often transduced by the same signaling components. We have used the *Saccharomyces cerevisiae* mating and filamentation mitogen-activated protein kinase (MAPK) pathways as a model system to study this problem of signaling specificity. While these pathways share multiple components, their distinct developmental programs are activated by different MAPKs: Fus3 functions in mating while Kss1 controls filamentous growth (Madhani et al. 1997).

The mating and filamentation MAPK pathways share two sets of components, one that acts upstream of the pathway-specific MAPKs and one that functions downstream (Fig. 1a). The first set of shared components includes the PAK (p20 activated kinase) Ste20, its target MEKK (MEK kinase) Ste11, and the MEK (MAPK/ERK kinase) Ste7. Depending on the input, Ste7 preferentially activates the pathway-specific MAPKs Fus3 or Kss1. Downstream of these pathway-specific components are the shared negative regulators Dig1 and Dig2. They bind and inhibit the shared transcription factor Ste12, which, depending on its DNA binding partner, is activated by either Fus3 or Kss1. This in turn induces the mating or filamentation gene transcription programs, respectively (Schwartz and Madhani 2004; Bardwell 2005). The structures of the pathways imply at least two mechanisms that prevent and/or suppress cross-talk, one for each set of shared components. One system would be responsible for activating the correct MAPK, while the other would ensure the activation of the appropriate gene set. Additionally, having more than one mechanism to ensure specificity might accommodate leakiness in any single mechanism.

We and others have recently identified one such specificity mechanism that functions downstream of the

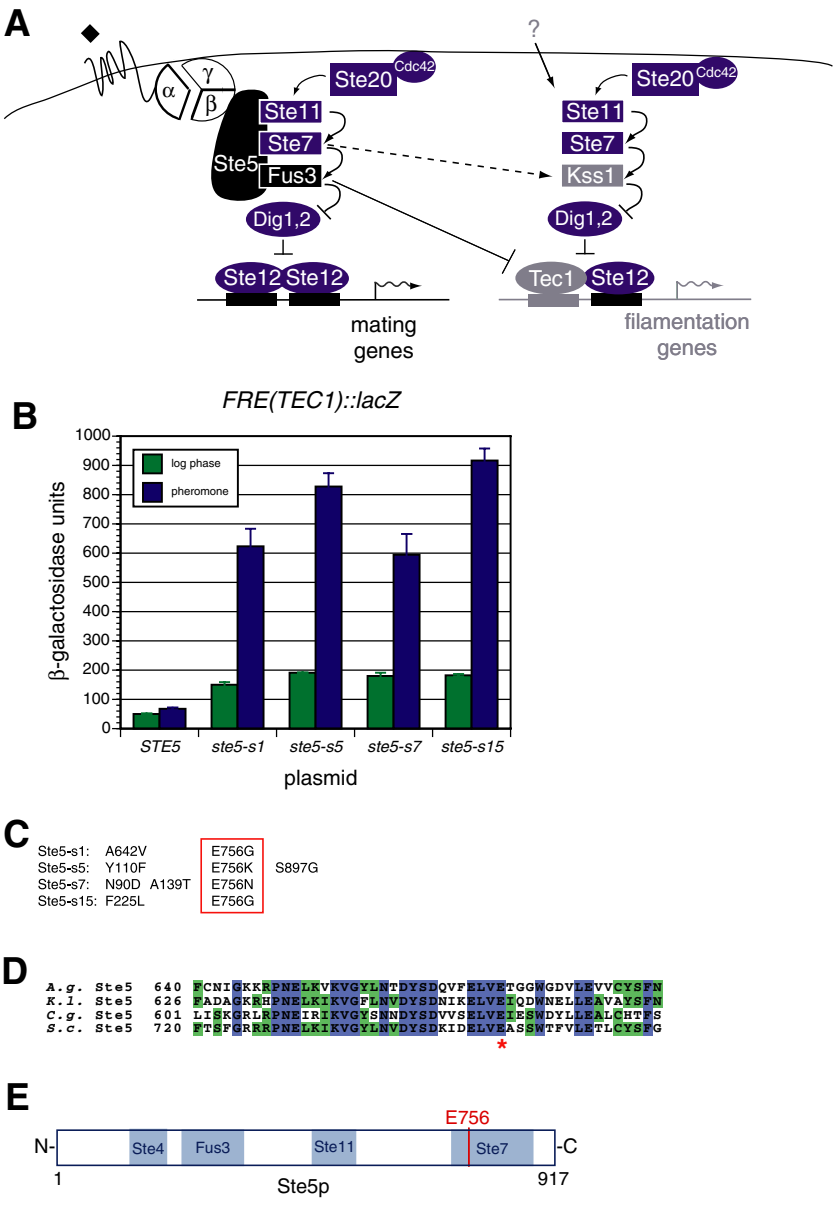

Fig. 1 Isolation of *STE5* cross-talk mutants. **a** Diagram of the mating and filamentation MAPK pathways in *S. cerevisiae*. Mating-specific components are shown in *black*, filamentation-specific components in *gray*, and shared components in *blue*. **b** *FRE(TEC1)::lacZ* expression. Shown are β-galactosidase activities of *ste5Δ* cells transformed with the indicated plasmids. Cultures were split and one sample was treated with α-pheromone for 2 h. **c** Mutations in four cross-talk alleles. **d** Alignment of amino acid sequences of Ste5 homologs of four ascomycete yeast species. Shown is a portion of the Ste7 binding domain of the homologs. *S.c. Saccharomyces cerevisiae, C.g. Candida glabrata, K.l. Kluyveromyces lactis, A.g. Ashbya gossypii. S. cerevisiae* E756 marked by *asterisk*. **e** Domain architechture of the multikinase scaffold Ste5. Indicated are the binding domains delineated in previous work and the approximate location of residue E756

MAPKs and seems to correct for leakage from an upstream mechanism (Bao et al. 2004; Bruckner et al. 2004; Chou et al. 2004). In response to pheromone, predominantly Fus3 is activated, but a fraction of Kss1 is as well. However, this fraction of Kss1 does not activate filamentation gene expression (Madhani et al. 1997). Active Fus3 phosphorylates the filamentation-specific transcription factor Tec1, which in turn induces the ubiquitin-dependent degradation of Tec1. Mutation of the site of Fus3 phosphorylation of Tec1 blocks its destruction and results in the erroneous activation of filamentation gene expression by pheromone signaling (Bao et al. 2004; Chou et al. 2004).

Scaffolding proteins, which are defined as proteins that tether two or more signaling components of a pathway, have been widely proposed to promote the specificity of signaling. However, whether they in fact prevent cross-talk between pathways that share components is not clear. In the pheromone response pathway, the Ste5 protein has been shown to bind Ste4 (the β subunit of the receptor–coupled heterotrimeric G protein), Ste11, Ste7, and Fus3 through largely non-overlapping binding domains (Choi et al. 1994; Marcus et al. 1994; Printen and Sprague 1994; Inouye et al. 1997; Elion 2001). Biochemical experiments have demonstrated that the activation of Fus3 depends critically on its association with Ste5 (Bardwell et al. 1996; Choi et al. 1999; Breitkreutz et al. 2001; van Drogen et al. 2001; Andersson et al. 2004; Maleri et al. 2004). In contrast, the evidence indicates that Kss1 does not associate with Ste5 nor does it require Ste5 for its activation. As is the case with other scaffolds, Ste5 has been proposed to not only promote the efficiency of signaling, but also specificity (Choi et al. 1994; Marcus et al. 1994; Printen and Sprague 1994).

However, whether Ste5 prevents cross-talk between the pheromone response pathways and other MAPK signaling pathways is unclear. Yashar et al. (1995) demonstrated that an activated allele of Ste7, Ste7-S368P could complement the defects produced by deletion of the genes encoding redundant MEKs of the yeast cell integrity MAPK pathway, but only in the absence of *STE5*. Although originally interpreted as evidence that Ste5 prevents cross-talk between the mating and cell integrity MAPK pathways (which do not share components), a later study showed that Ste7-S368P is non-specifically activated by a number of unrelated kinases (Inagaki et al. 1999). Thus the original results are more precisely interpreted as showing that Ste5 can inhibit either the promiscuous activation Ste7-S368P and/or its ability to phosphorylate the MAPK for the cell integrity pathway. Because of the unusual properties of the Ste7-S368P mutant, these studies do not speak directly to the function of Ste5 in the context of wild-type Ste7 and its activation during the course of the normal pheromone response.

Two other studies that addressed the role of Ste5 in signaling specificity used artificial protein fusions and focused on Ste11, the MEKK shared between three MAPK pathways, the mating, filamentation and high osmolarity glycerol (HOG) pathways. One group used an artificial hybrid scaffold that fused Ste5 and Pbs2 (scaffold and MEK for the HOG pathway) with mutations in the Ste7 and Sho1 (HOG pathway receptor) binding domains, respectively (Park et al. 2003). This fusion construct caused activation of the Hog1 MAPK and transcription of HOG genes in response to pheromone by transferring the mating signal from Ste11 to Pbs2 in the absence of Ste7 binding. Likewise, an earlier study demonstrated that it was possible to bias the outcome of signaling by fusing a shared component, such as Ste11, to a particular MAPK scaffold (Harris et al. 2001). For instance, a fusion of Ste11 to Ste5 activated promoter-*lacZ* reporters specific for the mating pathway, but not those specific to the filamentation or HOG pathways.

These results suggest that binding of the appropriate MAPK signaling pathway components to the scaffold, thereby increasing their local concentrations, can influence the outcome of signaling. However, they do not offer a rigorous test of whether specificity is maintained by the naturally-occurring scaffold and thus may not fully illuminate its normal mechanisms of action. In particular, permanently tethering components to the scaffold precludes the possibility that only the active forms are inhibited from dissociating from the scaffold and erroneously activating other pathways. Moreover, the efficiency of signaling was drastically reduced in some of these fusion constructs, further raising the possibility that the encoded fusion proteins did not recapitulate the activity of the corresponding natural scaffolds. Consistent with these caveats, a recent study by Bardwell and colleagues disputes the notion that Ste5 normally functions to sequester kinases from other pathways (Flatauer et al. 2005). Here we describe a genetic screen that identified a single residue in the Ste5 scaffold critical for the maintenance of signaling specificity.

Materials and methods

Construction of plasmid library of *STE5* mutations and screen for cross-talk mutants

A mutagenized pool of *STE5* was constructed by PCR amplification of 10 ng of the *Xba*I–*Bam*HI fragment containing *STE5* for ten cycles in a volume of 100 µl using Taq DNA polymerase and standard amplification conditions. This product was diluted 1:100 and used in a second round of amplification for ten cycles. This procedure was repeated until five rounds were completed. The product (1 µg) was digested with *Xba*I and *Bam* HI and ligated to 1 µg of *Xba*I/*Bam*HI-digested pRS316 (*URA3, CEN*) in a volume of 100 µl. The product was concentrated by precipitation with ethanol. The DNA was then resuspended in 10 µl ddH_20 and used to electroporate five aliquots of electrocompetent DH5α. Approximately 146,000 transformants were obtained. Blue/white screening indicated at least 99% of the transformants contained insert.

The plasmid library screening was transformed into a *ste5Δ* strain, containing a *CEN* plasmid expressing *FUS3* from the constitutive TPI promoter and a *FRE(Ty1)::lacZ* reporter gene on a 2 µm plasmid. The FUS3 plasmid was included to select against mutants that displayed cross-talk due to lower levels of FUS3 which was known previously to be sufficient to produce cross-talk. Inclusion of the plasmid resulted in lower reporter gene expression (data not shown). This accounts for the lower levels of reporter gene activity in Fig. 1b versus Fig. 2a. Tranformants were screened filter β-galactosidase method (Golemis and Khazak 1997). Yeast transformants were screened by replica-plating to plates containing no pheromone or to those spread with synthetic α-pheromone in DMSO.

Liquid β-galactosidase assays

Liquid β-galactosidase assays were performed using the freeze–thaw method as described (Bao et al. 2004). Error bars shown in figures depict standard deviations for three replicates. Because of day-to-day variation in values and degree of pheromone responses, all experiments described in a figure were performed on the same day. Analysis of data shown in Fig. 5a was done using Cyber-T (http://www.visitor.ics.uci.edu/genex/cybert/index.shtml). Confidence value for Bayesian variance estimate was set to 9).

Haploid invasive growth assay

Haploid invasive growth assays were performed by growing cells on YPAD solid for 3 days at 30°C

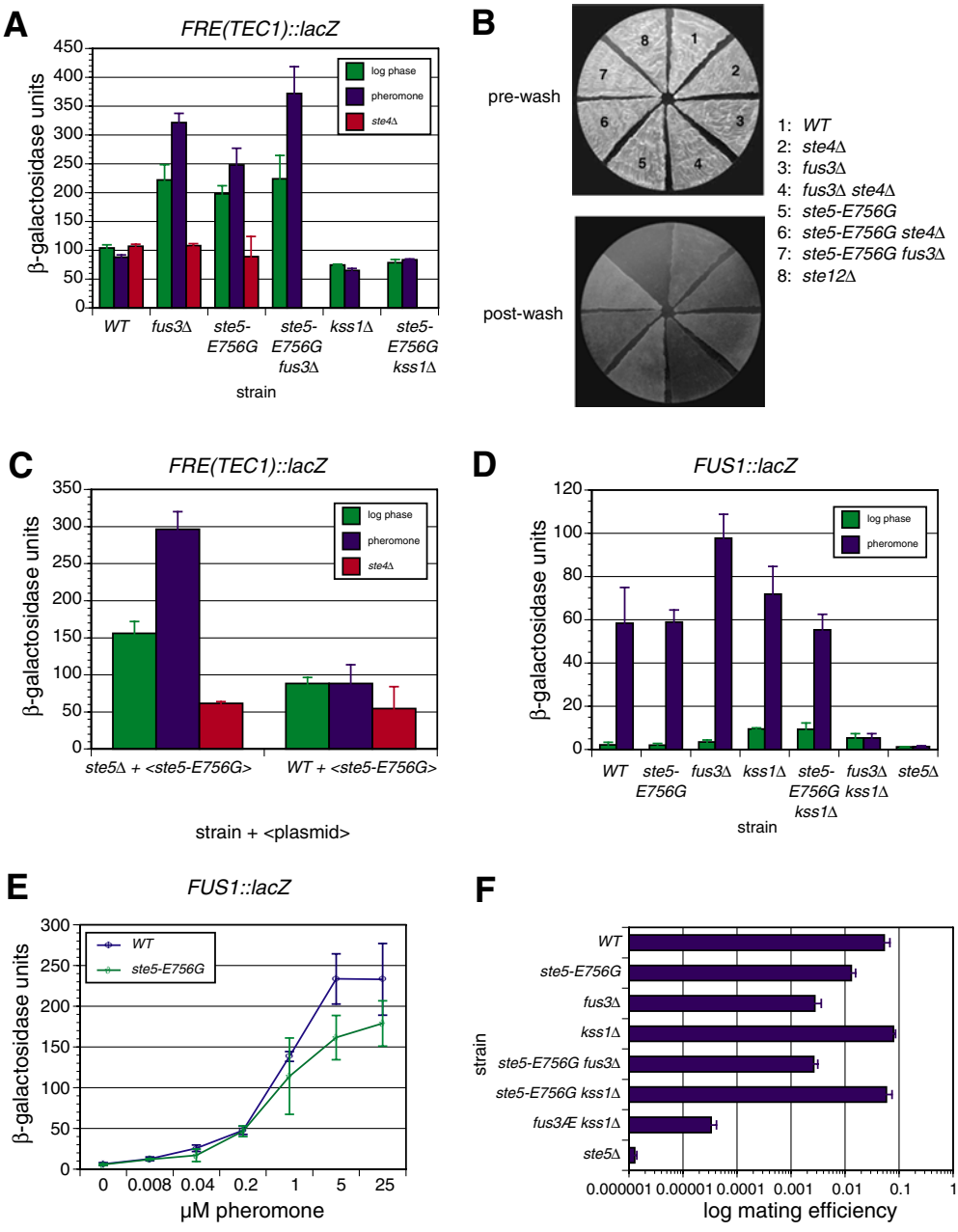

Fig. 2 Properties of the *ste5-E756G* mutant. **a** *FRE(TEC1)::lacZ* expression. Shown are β-galactosidase activities of indicated strains. Note that *kss1Δ ste4Δ* strains were not analyzed. **b** Haploid invasive growth assay. Shown is a YPAD plate after 2 days of growth at 30°C before and after washing under a stream of water. Yeast that have invaded the agar remain after the wash. **c** *FRE(TEC1)::lacZ* expression. Shown are β-galactosidase activities for *ste5Δ* and wild type strains transformed with a *ste5-E756G* centromeric plasmid. Cultures were split and one sample was treated with α-pheromone for 2 h. **d** *FUS1::lacZ* expression. Shown are β-galactosidase activities of indicated strains. Cultures were split and one sample was treated with α-pheromone for 2 h. β-galactosidase assay was performed. **e** Dose response curve of *FUS1::lacZ* expression. Shown are β-galactosidase activities of wild type and *ste5-E756G* treated for 2 h with the indicated pheromone concentration. **f** Quantitative mating assay. Averages and standard deviations triplicate samples are shown

followed by 2 days at room temperature followed by washing under a tap.

Quantitative mating

Triplicate cultures were grown to log phase. 2×10^6 cells of the indicated genotype were mixed with 1×10^7 cells of an α mating tester and collected on a nitrocellulose filter by vacuum filtration. Filters were placed on a YPAD plate and allowed to mate at 30°C for 5 h. Cells were washed off filter and plated in tenfold serial dilutions on media that selected for markers diagnostic of diploid mating products versus the haploid mating type **a** parent. Colonies were counted after one day of growth. Mating efficiency was calculated by the following formula: Diploid titer/(diploid titer + haploid titer). "Haploid titer" refers to the titer of the mating type **a** strain tested. Averages and standard deviations were calculated for the triplicate samples.

Extract preparation and immunoblotting

Cells were grown to mid-log phase (OD 0.6–0.8). The culture was split and half was treated with 5 μM α-pheromone for 15 min. Subsequent steps were carried out at 4°C. Cells (corresponding to 30–100 ml of culture) were lysed by 4×1.5 min agitation at maximum

speed in a Mini Bead Beater-8 (BioSpec Products) with zirconia/silica beads in lysis buffer-150 (150 mM NaCl, 50 mM Tris pH7.4, 5 mM EDTA, 1% NP-40, 50 mM NaF, 1 mM PMSF, 15 mM 4-nitrophenylphosphate, 30 mM $Na_2S_2O_5$, 0.1 mM Na_3VO_4, Sigma protease inhibitor cocktail, Sigma phosphatase inhibitor cocktails 1 and 2). Inhibitor cocktails were used at concentrations recommended by the manufacturer. Cell debris was removed by centrifugation at 14 K rpm for 10 min. Protein concentration was determined by a Bradford assay (BioRad). One hundred microgram of whole cell extract was resolved on 7.5 or 10% SDS-PAGE gels and transferred to nitrocellulose. Immunoblotting was performed with the following antibodies at the indicated dilutions: anti-p42/44 (1:1,000; NEB), anti-myc (1:1,000; 9E10, Covance), anti-Fus3 (1:1,000; a gift of Julie Brill), anti-Kss1 (1:2,000; a gift from Jeremy Thorner), anti-Ste7 (1:2,000; a gift from Brad Cairns), anti-phospho-Ste7 (1:1,000; custom generated at Phosphosolutions, Inc.), anti-FLAG (1:2,000; Sigma), anti-tubulin (1:2,000; Abcam), anti-mouse IgG-HRP (1:3,000; BioRad), anti-rabbit IgG-HRP (1:3,000; BioRad), anti-rat IgG-HRP (1:3,000; Jackson Laboratories). Membranes were stripped by incubation 0.2 M NaOH for 5 min and reprobed where indicated.

For time course experiments, cells were grown to mid-log phase, induced with 5 μM α-pheromone and collected at the indicated time points. Cells (corresponding to 25 ml of initial culture) were lysed in 3 μl Y-PER (Pierce) per OD of cells at room temperature for 15 min. Cell debris was removed by centrifugation at 14 K rpm for 10 min. Equivalent amounts of extract were loaded and immunoblotting was performed as above.

Velocity sedimentation analysis

Step gradients were poured in 5×1 ml steps of 30–10% glycerol prepared in lysis buffer-150 in 13×51 mm Polyallomer tubes (Beckman). Extracts from log phase cells were prepared as above in lysis buffer-250 (250 mM NaCl, otherwise same as lysis buffer-150). Bradford assays (BioRad) were performed to determine protein concentration. Extracts containing 1 mg of protein was layered on top of the gradient. Gradients were centrifuged at 43 K rpm at 4°C for 12 h in a Beckman SW55 rotor. Markers were subjected to centrifugation in parallel. Fifteen fractions were collected from the top by a Foxy Jr. fraction collector. Fractions were precipitated by addition of TCA to 10%. Pellets were solubilized in 8 M urea, sample buffer was added and the solubilized fractions were boiled for 5 min. The samples were loaded on a 7.5% Tris–HCl gel. Membranes were probed with anti-Ste7 antibody. The membranes were stripped with 0.2 M NaOH and reprobed with anti-FLAG antibody.

Results

To test the role of a naturally-occurring signaling scaffold in pathway fidelity, we performed a screen for *STE5* loss-of-specificity mutants. Four strong cross-talk alleles were isolated that displayed basal hyperactivation of an *FRE(TEC1)::lacZ* filamentation response element-containing reporter (Madhani and Fink 1997) and further activation in response to pheromone treatment (Fig. 1b). While all four alleles had multiple mutations, they shared a change in a single amino acid: glutamate 756. This residue was mutated to one of three different residues, glycine, lysine or asparagine (Fig. 1c). This residue is invariant in Ste5 homologs in ascomycete fungi in which we could identify clear homologs of Ste5 (Fig. 1d). Interestingly, this residue is in a domain of Ste5 that binds the MEK Ste7 (Inouye et al. 1997), a pathway component that is shared between the mating and filamentation pathways (Fig. 1e).

We constructed the *ste5-E756G* single mutation and replaced the chromosomal *STE5* with this allele. A reporter assay measuring *FRE(TEC1)::lacZ* activity demonstrated that basal signaling through the filamentation pathway was increased and signaling was further induced after pheromone treatment (Fig. 2a). This increased level of signaling returned to wild-type levels when mating pathway signaling was eliminated by the removal of Ste4, the pheromone pathway-specific Gβ subunit. Thus, the *ste5-E756G* mutation was sufficient to cause cross-talk. A *ste5-E756G fus3Δ* mutant displayed a similar phenotype to either single mutant. The cross-talk phenotype was lost in a *ste5-E756G kss1Δ* double mutant indicating that the loss of specificity requires Kss1. We measured haploid invasive growth to test a biological output of the filamentation pathway. As expected, plate-washing assays showed that, like *fus3Δ*, *ste5-E756G* is hyperinvasive in a *STE4*-dependent manner (Fig. 2b).

To rule out the possibility that *ste5-E756G* was a gain-of-function mutation that could now act in both the mating and filamentation pathways, we tested whether the mutant allele was dominant or recessive. While *ste5-E756G* caused cross-talk when expressed alone, the addition of wild-type *STE5* expression prevented perturbations of the mating pathway from influencing the filamentation pathway (Fig. 2c), indicating that the scaffold mutant is recessive.

We next measured the efficiency of signaling through the mating pathway using a *FUS1::lacZ* reporter assay (McCaffrey et al. 1987). In *ste5-E756G* cells, signaling through the mating pathway was very similar to wild type (Fig. 2d). In a dose-response experiment revealed no significant difference in maximal reporter gene activation in the mutant (Fig. 2e). To measure the biological output of this pathway, we performed quantitative mating measurements (Fig. 2f) and found that *ste5-E756G* displayed a mild mating defect. Mating efficiency was reduced by approximately one log unit compared to

wild type, but was reproducibly slightly higher than a *fus3Δ* strain. Surprisingly, removal of the filamentation MAPK Kss1 rescued the mating defect of *ste5-E756G* while deletion of both *FUS3* and *KSS1* caused sterility, as previously observed (Elion et al. 1991). This result hinted at a competition between the MAPKs for activation by Ste7 in the *ste5-E756G* mutant.

To gain insight into the mechanisms by which the *ste5-E756G* mutation caused cross-talk, we assessed the level of Fus3 and Kss1 phosphorylation using a mammalian anti-p44/42 antibody, which specifically detects Fus3 and Kss1 phosphorylated on their activation loops (Sabbagh et al. 2001). In *ste5-E756G* cells, the basal level of Kss1 phosphorylation was reproducibly higher than in wild type (Fig. 3a). Upon pheromone addition, Kss1 showed increased phosphorylation compared to wild-type, like in a *fus3Δ* strain (Fig. 3a; see also Fig. 5b, lanes 7 and 8). The mutant scaffold also displayed a dramatic decrease in the phosphorylation of Fus3. Strikingly, when *KSS1* was deleted in the scaffold mutant background, the defect in Fus3 activation was greatly reduced (Fig. 3a). In contrast, kinase-dead Kss1 did not rescue Fus3 activation in the *ste5-E756G* background (unpublished observations), again suggesting that Kss1 and Ste5 may compete for active Ste7. Although Fus3 levels increase by 15 min in pheromone treated cells (presumably due to the fact that the *FUS3* promoter is itself regulated by the pheromone response pathway), the relative increase appears to be the same for wild-type and mutant strains; thus, the changes in phosphorylation level are not due to differences in the steady-state levels of Fus3 or Kss1 (Fig 3b). This change in MAPK activation pattern in the *ste5-E756G* cells was recessive to wild type (Fig. 3c). Consistent with these results and the location of the E756G mutation in the Ste7 binding domain, co-immunoprecipitation experiments using overexpressed derivatives showed that Fus3 associated with both wild-type and mutant version of Ste5 (unpublished observations).

Since the E756G mutation is in the Ste7 binding domain of Ste5, a simple hypothesis is that this mutation affects binding of Ste7 to Ste5. We therefore performed *FRE* reporter assays with a previously isolated Ste5 mutant with reduced binding to Ste7, Ste5-D746G (Inouye et al. 1997) (Fig. 4a). We found that the filamentation signaling in this mutant was unaffected by perturbations of the mating pathway. Additionally, *ste5-D746G* displayed wild-type levels of Fus3 phosphorylation and a moderate increase in Kss1 phosphorylation (Fig. 4b). We hypothesize that this increased Kss1 phosphorylation did not cause cross-talk because there was sufficient active Fus3 to maintain specificity by causing degradation of Tec1 (Bao et al. 2004; Bruckner et al. 2004; Chou et al. 2004). Thus, a modest reduction in binding of Ste7 to the scaffold is not sufficient to cause measurable cross-talk. In contrast, we found that *ste5-VASP* (V763A S861P) (Inouye et al. 1997), an allele that displays no detectable binding to Ste7, yielded low levels

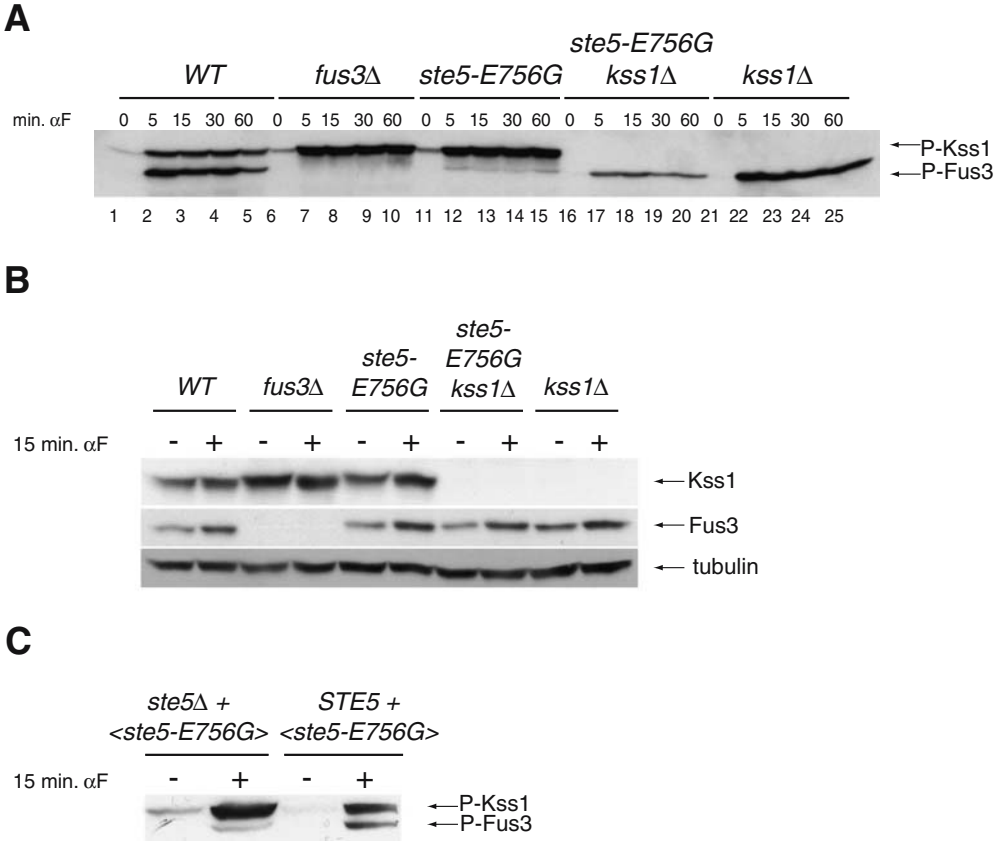

Fig. 3 Analysis of MAPK activation and levels in wild-type versus *ste5-E756G* cells. **a** Time course of Fus3 and Kss1 phosphorylation. Shown is an immunoblot using anti-phospho-MAP kinase antibodies of the indicated strains collected at the indicated times after treatment with α-pheromone. **b** Fus3 and Kss1 proteins levels. Shown is an immunoblot analyzing the steady-state levels of Fus3 and Kss1 in the indicated strains. α-tubulin served as a loading control. **c** Fus3 and Kss1 phosphorylation levels of the indicated strains

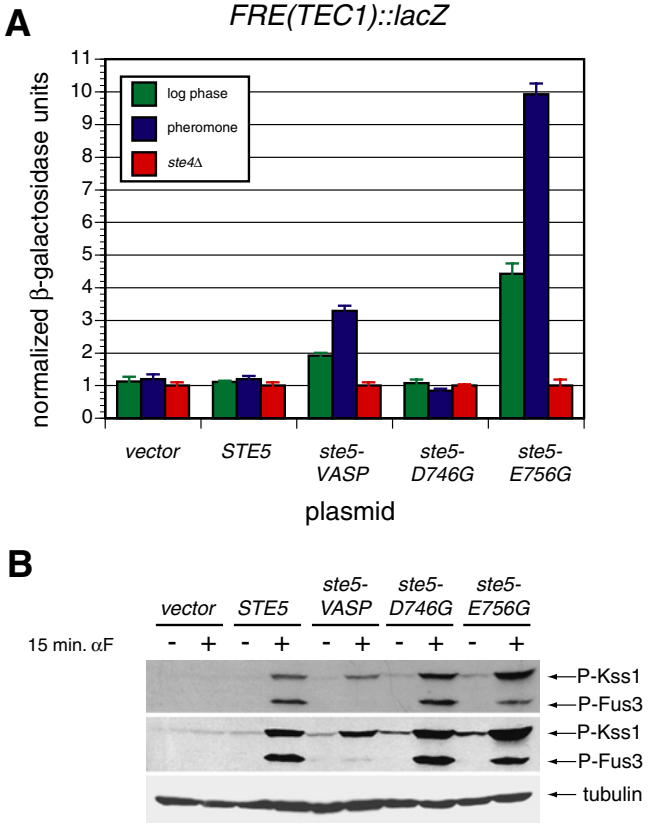

Fig. 4 Characterization of Ste7-binding mutants of Ste5. **a** Normalized *FRE(TEC1)::lacZ* expression. Shown are *β*-galactosidase activities of *ste5Δ* cells transformed with the indicated plasmids normalized to the respective *ste4Δ* strain. Cultures were split and one sample was treated with *α*-pheromone for 2 h. *β*-galactosidase activities were normalized to their respective *ste4Δ* strains because plasmids carrying *ste5* alleles were on different vector backbones, resulting in different copy numbers and levels of basal reporter expression. **b** Fus3 and Kss1 phosphorylation levels of the indicated strains. Second panel, longer exposure of same blot to visualize Fus3 phosphorylation in *ste5-VASP*. *α*-tubulin served as a loading control

of cross-talk compared to *ste5-E756G* (Fig. 4a). Upon pheromone addition, *ste5-VASP* shows virtually no induction of Fus3 phosphorylation, and a modest increase in Kss1 phosphorylation (Fig. 4b). We propose that the low levels of Kss1 activation can only cause minimal cross-talk, despite having a defect in Fus3 phosphorylation.

To determine the role of Fus3-dependent Tec1 degradation in *ste5-E756G*, we compared the levels of cross-talk in the scaffold mutant and in a mutation in the Fus3 phosphorylation site of Tec1 (*tec1-T273M*) (Bao et al. 2004; Bruckner et al. 2004; Chou et al. 2004). The *ste5-E756G tec1-T273M* double mutant reproducibly displayed significantly higher levels of cross-talk than either single mutant (Fig. 5a; Bayes $P < 1.8\times10^{-4}$ for pheromone-treated double mutant vs. *tec1-T275M* and $P < 5.6\times10^{-5}$ for pheromone-treated double mutant vs. *ste5-E756G*). To determine how this increased level of cross-talk was generated, we examined Tec1 protein levels and the phosphorylation of the MAPKs in response to pheromone (Fig. 5b). Some Tec1 degradation was observed in the scaffold mutant but to a reproducibly lesser extent than in wild type (Fig. 5b, lanes 9 and10 vs. lanes 3 and 4), presumably due to the incomplete defect in Fus3 activation. In contrast, Kss1 phosphorylation levels remained unchanged in the *tec1-T273M* mutant, while Kss1 shows increased phosphorylation in the *ste5-E756G* mutant compared to either wild-type of the *tec1-T273M* mutant (Fig. 5b, lane 8 vs. lanes 2,3 or 6). These data suggest two sources for the specificity defect of *ste5-E756G*; one is the defect in degradation of Tec1, while a second mechanism caused the hyperactivation of Kss1.

To explain the properties of the *ste5-E756G* mutant, we hypothesized that the E756G mutation caused frequent dissociation of an active subpopulation of Ste7 from Ste5, while this occurred rarely in wild-type cells (Fig. 6a). To test this model, we sedimented whole cell extracts from wild type and mutant cells with and without pheromone treatment through a 10–30% glycerol gradient. Previous gradient analyses of extracts have shown that a fraction of Ste7 molecules associate with a high molecular weight complex of Ste5 that also contains Ste11 and Fus3 (Choi et al. 1994). This complex is highly enriched for Fus3 kinase activity and sediments at a molecular weight of 350–500 kD (Choi et al. 1999).

Ste7 occurs in two electrophoretic forms (Zhou et al. 1993; Errede and Ge 1996). The slower migrating form, here termed Ste7-ret-P, is induced by signaling through the mating and filamentation pathways, and is thought to represent Ste7 that is retrograde-phosphorylated by Fus3 and Kss1 (Zhou et al. 1993; Errede and Ge 1996). The faster migrating species is not retrograde phosphorylated. In untreated cells, two sedimentation peaks of Ste7 were observed after immunoblotting of gradient fractions with a polyclonal antibody against Ste7 (Fig. 6b), which we refer to as the low (fractions 7–9) and high molecular weight forms (fractions 11–15). The high molecular weight form corresponds to the Ste7 population complexed with the scaffold based on its molecular weight, and the observation that a population of Ste5 reproducibly co-sedimented with Ste7 in this region of the gradient (unpublished observations). In the absence of induction, both molecular weight forms consisted primarily of Ste7 that was not retrograde-phosphorylated (Fig. 6b, log phase).

Extracts from pheromone-treated wild-type cells displayed an increase in the retrograde phosphorylated form of Ste7 (Fig. 6b, compare log phase to 15 min αF). Importantly, this retrograde phosphorylated population of Ste7 is found predominately in the higher molecular weight complex. This suggests Ste7-ret-P is mainly associated with the scaffold complex in wild type cells. The association of both Ste7 and Ste7-ret-P in the high molecular weight complexes is consistent with an earlier study which demonstrated that both populations of Ste7 co-immunoprecipitate with Ste5 (Sette et al. 2000). We note that other studies that examined overexpressed, C-

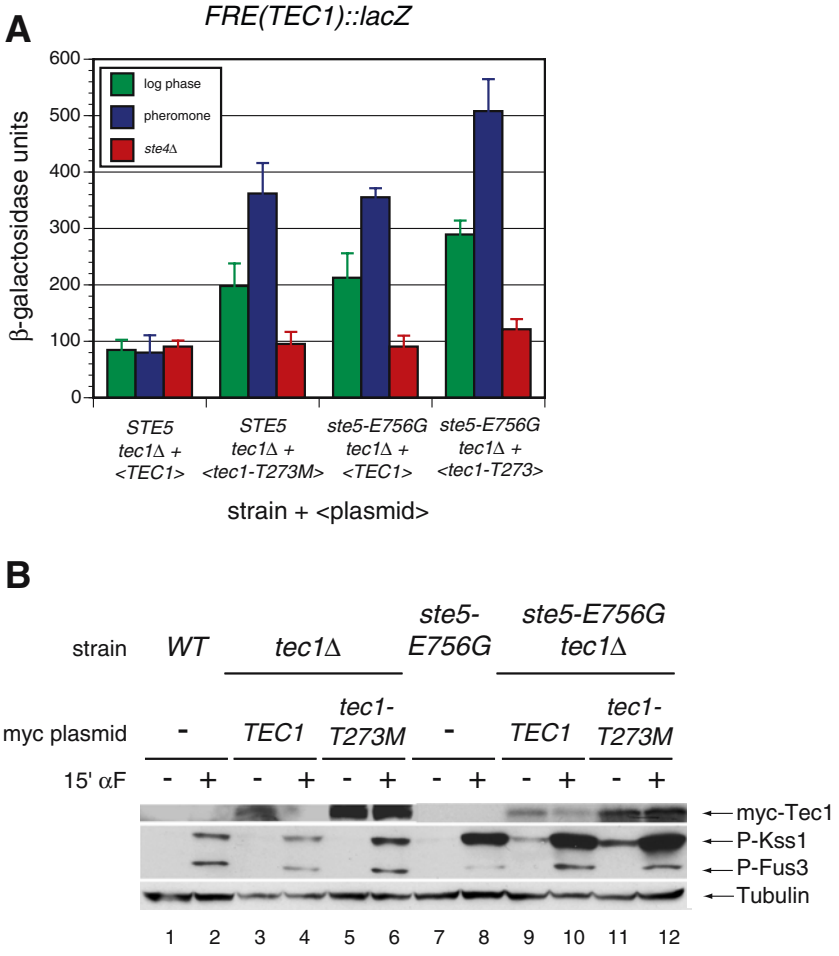

Fig. 5 Analysis of the mechanisms of cross-talk in *ste5-E756G* cells. **a** *FRE(TEC1)::lacZ* expression. Shown are β-galactosidase activities of the indicated strains. Cultures were split and one sample was treated with α-pheromone for 2 h. **b** Tec1 protein levels and MAPK phosphorylation levels. Shown is an immunoblot of the indicated strains probed with anti-myc to determine Tec1 levels. Tec1 levels in the *ste5-E756G* background (*lanes 7–12*) were higher than in the wild type background. The exposure time shown for anti-myc in the wild type background (*lanes 1–6*) is approximately 20 times longer. The blot was stripped and reprobed with the anti-p42/44 antibody to assay Fus3 and Kss1 phosphorylation. The membrane was again reprobed with anti-tubulin as a loading control

terminally tagged Ste7 concluded that the retrograde-phosphorylated form of Ste7 binds poorly to Ste5 (Choi et al. 1994; Maleri et al. 2004), but another study showed that disruption of the C-terminus causes a loss of Ste7 function (Sabbagh et al. 2001). Our studies differ in that they examine the endogenous protein.

In pheromone-treated *ste5-E756G* cells, we observed a depletion of Ste7-ret-P from the scaffold-associated complex in the high molecular weight fractions (compare Fig. 6c to b, 15 min αF). Additionally, we observed an increase in this retrograde phosphorylated form of Ste7 in the low molecular weight form. Thus, a specific subpopulation of phosphorylated Ste7 appeared to be dissociated from the mutant scaffold.

To determine whether this retrograde phosphorylated form of Ste7 was activated, we blotted whole cell extracts with antibodies raised against a phosphopeptide corresponding to the phosphorylated activation loop of Ste7. We observed a pheromone- and Ste11-dependent signal upon immunoblotting (Fig. 6d). Re-probing of the blot with polyclonal anti-Ste7 antibodies revealed that the retrograde-phosphorylated form of Ste7 also contained Ste7 phosphorylated on its activation loop, whereas the non-retrograde-phosphorylated species was devoid of activated Ste7 (Fig. 6d). This suggests that in *ste5-E756G*, the Ste7 population that displayed a shift from the complexed form toward the lower molecular weight form contained activated Ste7. Retrograde phosphorylation of Ste7 in the Ste5 mutant occurred in cells harboring kinase-dead Kss1 (unpublished observations), suggesting that Fus3 could phosphorylate Ste7 in *ste5-E756G* cells.

We were precluded from directly probing gradient fractions with the anti-phospho-Ste7 antibody because we observed lower levels of steady-state Ste7 phosphorylation in extracts made from *ste5-E756G* cells (unpublished observations). Although this could reflect decreased initial activation of Ste7 in the mutant, given the rapid kinetics of MAPK phosphorylation in the mutant, we favor the alternative explanation that Ste7 dissociated from the scaffold is more susceptible to dephosphorylation in vivo and/or in vitro. However, our data do not distinguish between these possibilities.

Discussion

Do signaling scaffolds promote specificity?

Ste5 was the first scaffold protein identified that tethers multiple kinases (Choi et al. 1994; Marcus et al. 1994; Printen and Sprague 1994). Since then, at least 18 scaf-

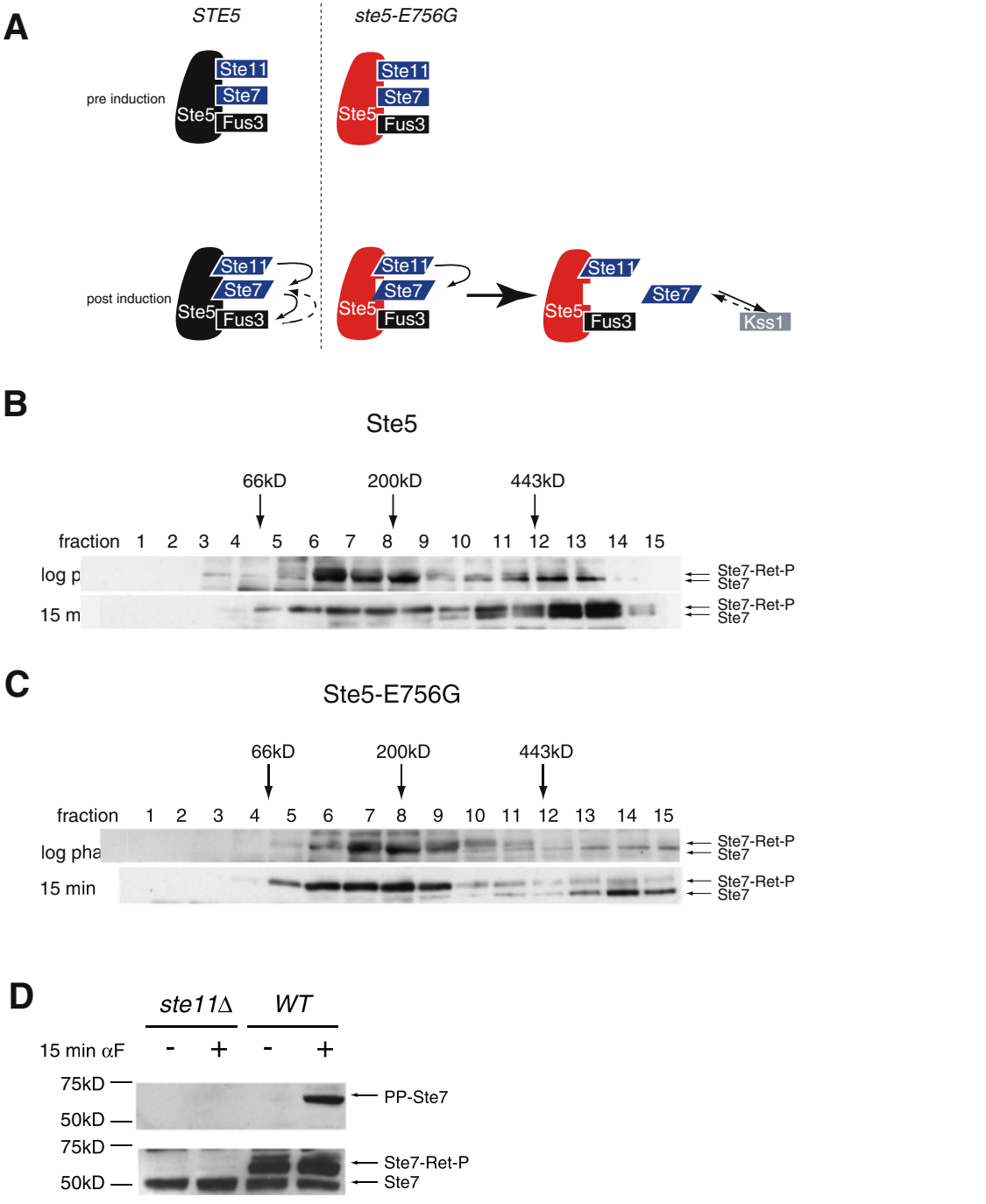

Fig. 6 A phosphorylated subpopulation of Ste7 appears dissocated from the Ste5-E756G scaffold. **a** Model of the role of Ste5 in signaling specificity. Mating-specific components are indicated in black, filamentation-specific components in *grey*, shared components in *blue*, mutant component in *red*. Active kinases indicated by parallelograms. *Dotted lines* indicate retrograde phosphorylation. Prior to induction, Ste7 binds to the scaffold, but can dissociate at a moderate rate. We propose that once Ste7 has been activated, it rarely dissociates because it is in a conformation that binds to Ste5 differently—indicated by a differently shaped fit between active Ste7 and Ste5. This distinct binding mode requires contacts between E756 and Ste7. The *ste5-E756G* mutant (shown in *red*) has a similar affinity for inactive Ste7. However, once Ste7 is activated, the enhanced binding is lost, because the binding site in Ste5 for activated Ste7 is disrupted by the mutation of E756. Activated Ste7 dissociates rapidly resulting in decreased activation of Fus3 and increased activation of Kss1, leading to cross-talk. **b** Immunoblot of gradient fractions. Extracts were prepared from a tagged *STE5* strain (*STE5-3FLAG*) with and without 15 min. of α-pheromone treatment. Fraction 1 is from the top of the gradient, 15 from the bottom. **c** Immunoblot of gradient fractions. Extracts were prepared from *ste5-E756G-3FLAG* strain. **d** Activated Ste7 is present exclusively in retrograde phosphorylated population. Immunoblot of indicated strains probed with the phospho-specific anti-PP-Ste7 antibody (specific to activation loop phosphorylations), stripped and reprobed with polyclonal anti-Ste7 antibody (*bottom panel*)

fold proteins associated with mammalian MAPK cascades have been described (Morrison and Davis 2003). Moreover, scaffolds have been identified in numerous other types of signaling systems, further emphasizing their importance. Upon the recognition of its scaffold function, Ste5 was proposed to promote not only the efficiency of signaling, but also the specificity (Choi et al. 1994; Marcus et al. 1994; Printen and Sprague 1994). In particular, it was hypothesized that Ste5 insulates the pheromone response MAPK pathway from other pathways with which it shares components. This original proposal has been broadly extended to many other signaling scaffolds (Hall and Lefkowitz 2002).

In the case of yeast MAPK signaling pathways, evidence in favor of the hypothesis that scaffolds promote specificity has been derived primarily from experiments in which various chimeric proteins were expressed in vivo. These experiments demonstrated that tethering a kinase to a scaffold (Harris et al. 2001) or fusing two scaffolds (Park et al. 2003) can direct the outcome of signaling. As described in the introduction, such constructs are artificial covalent fusions, which makes the application of the results to normal physiology problematic. Moreover, other studies have argued against a role for Ste5 in preventing the erroneous activation of other pathways (Flatauer et al. 2005). Because of these issues, we chose to study the function of a natural scaffold.

We sought point mutations in the Ste5 scaffold that produce a loss of signaling specificity. Remarkably, random mutagenesis of the *STE5* ORF followed by genetic screening yielded multiple independent mutants that shared changes in a single conserved amino acid, E756. These mutants produced a high degree of cross-talk with the filamentous growth MAPK pathway. To our knowledge, these are the first mutations reported in a natural signaling scaffold that cause a defect in the insulation of pathways from each other.

Characterization of the *ste5-E756G* mutant

Our characterization of the *ste5-E756G* single mutant revealed that it was sufficient to produce robust cross-talk, indicating that the other changes present in the alleles identified in the original screen were not required for the fidelity phenotype. We found that this mutation is a recessive loss-of-function allele. The dominance of the wild-type allele may be explained by the co-localization and potential dimerization of the wild type and mutant scaffolds at the mating projection (Yablonski et al. 1996; Mahanty et al. 1999; Sette et al. 2000; van Drogen et al. 2001). Thus we propose that when the activated Ste7 dissociates from the mutant scaffold, it is be rapidly and tightly re-bound by the wild-type Ste5, which would favor activation of Fus3 over Kss1. Additionally, our data suggest that the mutant scaffold is active in signaling. The induction of the pheromone pathway-specific reporter *FUS1::lacZ* was similar to wild type even when cells were treated with limiting amounts of mating pheromone, and the scaffold mutant displayed only a mild defect in mating efficiency.

Supporting the view that *ste5-E756G* cells still display efficient signaling, cells containing the mutant scaffold demonstrated rapid induction in response to mating pheromone, as assayed by the levels and kinetics of Fus3 and Kss1 phosphorylation. Maximal phosphorylation was obtained within five minutes in both wild type and mutant cells, and signaling appeared to be equally sustained in the two cases. However, *ste5-E756G* cells displayed a shift in the relative amounts of Fus3 and Kss1 phosphorylation, while binding to wild-type levels of Fus3. Increased maximal phosphorylation of Kss1 and a defect in the phosphorylation of Fus3 were observed. Because Fus3 promotes specificity by inducing the degradation of Tec1, and Kss1 is the MAPK for the filamentous growth pathway, it seems very likely that these changes in the pattern of MAPK activation cause the cross-talk phenotype of mutations in E756. To gain additional insight, we investigated two mechanistic questions: (1) what are the mechanisms by which this shift leads to cross-talk between the mating and filamentous growth MAPK pathways?, and (2) how does the *ste5-E756G* mutation lead to a shift in the pattern of MAPK activation?

Increased Kss1 activation and a defect in Tec1 degradation contribute to the *ste5-E756G* cross-talk phenotype

We and others have previously demonstrated that Fus3 suppresses cross-talk by phosphorylation of the filamentation-specific transcription factor Tec1, causing its subsequent degradation (Bao et al. 2004; Chou et al. 2004). In the absence of this mechanism, the fraction of Kss1 activated in response to mating pheromone inappropriately activates the filamentation transcriptional program. Since the *ste5-E756G* mutant is defective in the phosphorylation of Fus3 in response to mating pheromone, one possibility was that some or all of the specificity defect of the scaffold mutant was due to a defect in Tec1 degradation. To address this issue, we took advantage of a degradation-resistant phosphorylation site mutant in Tec1, *tec1-T273M*.

Our analysis of the *ste5-E756G tec1-T273M* double mutant revealed a small but reproducible increase in cross-talk as compared to either single mutant. This increase can be explained by the difference between the biochemical phenotypes of *ste5-E756G* and *tec1-T273M*. The former caused a large increase in Kss1 activation while the latter did not. Combining the two mutations resulted in hyperactivation of Kss1, which allowed more Tec1 to be activated and none to be degraded by Fus3, producing higher levels of cross-talk than either single mutant. The cross-talk phenotype of *ste5-E756G* is therefore due to a both defect in the degradation of Tec1 and an increase in Kss1 phosphorylation.

Table 1 *Saccharomyces cerevisiae* strains used in this study

Gentoype	Strain #
*MAT***a** *ura3 leu2 trp1 his3*	F1950
*MAT***a** *ste4::HIS3MX6 ura3 his3 trp1 leu2*	YM1622
*MAT***a** *ste5-E756G ura3 his3 trp1 leu2*	YM2181
*MAT***a** *ste5-E756G ste4::nat^{R}MX4 ura3 his3 trp1 leu2*	YM1692
*MAT***a** *fus3::HIS3MX6 ura3 his3 trp1 leu2*	YM1637
*MAT***a** *fus3::LEU2 ste4::nat^{R}MX4 ura3 leu2 trp1 his3*	YM1691
*MAT***a** *ste5-E756G fus3::nat^{R}MX4 ura3 leu2 trp1 his3*	YM2182
*MAT***a** *ste5-E756G kss1::nat^{R}MX4 ura3 leu2 trp1 his3*	YM2183
*MAT***a** *kss1::nat^{R}MX4 pPGU1::TRP1 ura3 his3 trp1 leu2*	YM1395
*MAT***a** *kss1::hisG fus3::TRP1 ura3 leu2 trp1 his3*	YM107
*MAT***a** *ste12::HIS3MX6 ura3 leu2 trp1 his3*	YM1638
*MAT***a** *ste5::HIS3 ura3 leu2 trp1 his3*	L6280
*MAT***a** *ste5::HIS3 ste4::nat^{R}MX4 ura3 leu2 trp1 his3*	YM1644
*MAT***a** *tec1::kan^{R}MX6 ura3 his3 trp1 leu2*	YM1934
*MAT***a** *tec1::kan^{R}MX6 ste4::nat^{R}MX4 ura3 his3 trp1 leu2*	YM1935
*MAT***a** *ste5-E756G tec1::HIS3MX6 ura3 his3 trp1 leu2*	YM2019
*MAT***a** *ste5-E756G tec1::HIS3MX6 ste4::nat^{R}MX4 ura3 his3 trp1 leu2*	YM2020
*MAT***a** *STE5-3FLAG-kan^{R}MX6 pep4::nat^{R}MX4 ura3 his3 trp1 leu2*	YM1842
*MAT***a** *ste5-E756G-3FLAG- kan^{R}MX6 pep4::nat^{R}MX4 ura3 his3 trp1 leu2*	YM1843
MATα his1 (mating tester)	17/17
∑1278b strain background	

Increased dissociation of active Ste7 may account for the shift in MAPK activation

The E756G mutation lies in a domain of Ste5 required for its binding to Ste7. Inouye et al. (1997) used a reverse two-hybrid approach to identify four mutations that contain changes in this domain and disrupt the interaction between Ste5 and Ste7. Among these was *ste5-D746G*, a mutation that weakens, but does not eliminate the scaffold–kinase association. We found that this mutation did not produce a cross-talk phenotype, suggesting that E756G is not an analogous mutation. Indeed, the fact that mutations in E756 were isolated repeatedly in our screen, and that our data demonstrates normal mating and MAPK activation kinetics, suggests that this residue plays a more specific role.

Correspondingly, our sedimentation analysis of extracts prepared from wild type and mutant scaffold strains indicated that a phosphorylated subpopulation of Ste7 is dissociated from the mutant scaffold. This subpopulation is a slower migrating electrophoretic form of Ste7 that was shown previously to be the result of retrograde phosphorylation by Fus3 or Kss1 (Zhou et al. 1993; Errede and Ge 1996). Our analysis demonstrated that this population also contained Ste7 phosphorylated on the activation loop. Together, these data suggest that the scaffold mutation causes an increase in the dissociation of activated Ste7.

How does the increased dissociation of active Ste7 from the mutant Ste5 lead to a decrease in Fus3 activation and an increase in Kss1 activation? Numerous studies indicate that in contrast to Fus3, the activation of Kss1 does not require association with Ste5 and furthermore, that Kss1 does not associate with Ste5 in vivo (Bardwell et al. 1996; Breitkreutz et al. 2001; van Drogen et al. 2001; Andersson et al. 2004; Flatauer et al. 2005). Given the opposite requirements for Ste5 for the activation of Fus3 and Kss1, a high rate of dissociation of active Ste7 from the scaffold should lead to decreased activation of Fus3 and increased activation of Kss1. This is precisely what is observed experimentally for the *ste5-E756G* mutant (Fig. 4a). Our genetic data provided additional support for this model. Cells expressing the mutant scaffold displayed a mild mating defect and a strong defect in the activation of Fus3. Both of these phenotypes were suppressed by the deletion of *KSS1*, consistent with the notion of an in vivo competition between Ste5 and Kss1 for active Ste7.

How might E756 accomplish a specific role in tethering the active Ste7 kinase to the scaffold? Ste7, once phosphorylated and catalytically active, may be in a different conformation than inactive Ste7 (Fig. 6a). Although crystal structures of MEKs comparing active and inactive conformations are not available, studies of numerous other kinases, including MAPKs, demonstrate conformational changes associated with kinase activation. It is therefore feasible that those two species of Ste7 make different contacts with the scaffold (as modeled in Fig. 6) (Tables 1, 2). We hypothesize that the function of E756 is to form part of a binding site that is specific for the active form of Ste7. While structural studies will ultimately be required to test this idea rigorously, it provides a useful framework for understanding the mechanism by which Ste5 might promote specificity. E756 is invariant among species with identifiable homologs of Ste5, suggesting that the maintenance of specificity by this residue is under evolutionary pressure. Additionally, there is evidence that the differential binding of Ste5 to active kinases might apply to its other partners: Photobleaching studies of Fus3-GFP dynamics in vivo showed that once phosphorylated, Fus3 is released more rapidly from the plasma membrane of

Table 2 Plasmids used in this study

Plasmid name	Centromere	Marker	Strain #
ste5-s1	*CEN/ARS*	*URA3*	BHM561
ste5-s5	*CEN/ARS*	*URA3*	BHM562
ste5-s7	*CEN/ARS*	*URA3*	BHM563
ste5-s15	*CEN/ARS*	*URA3*	BHM569
TPI-FUS3	*CEN/ARS*	*TRP1*	B3819
Ty1::lacZ	2 μ	*URA3*	BHM261
pRS316-ste5-E756G	*CEN/ARS*	*URA3*	BHM853
FRE(TEC1)::lacZ	2 μ	*URA3*	BHM275
pFUS1::lacZ	2 μ	*URA3*	BHM859
YCp-50	*CEN/ARS*	*URA3*	B489
YCp-HIS6-myc-STE5	*CEN/ARS*	*URA3*	BHM806
YCp-HIS6-myc-ste5-VASP	*CEN/ARS*	*URA3*	BHM808
YCp-HIS6-myc-ste5-D746G	*CEN/ARS*	*URA3*	BHM807
kss1-K42R	*CEN/ARS*	*HIS3*	BHM454
6myc-TEC1	*CEN/ARS*	*URA3*	BHM969
6myc-tec1-T273M	*CEN/ARS*	*URA3*	BHM1055

mating projections where it is presumably bound to Ste5 (van Drogen et al. 2001).

Although the model presented is consistent with our data and the available literature, we cannot rule out the possibility that the retrograde phosphorylated form of Ste7 also contains inactive Ste7. It is therefore possible that the altered gradient migration pattern of retrograde phosphorylated Ste7 represents the inactive population of Ste7, and that the active form selectively stays bound to the mutant scaffold. Nonetheless, given the location of the mutation, the switch in MAPK activation pattern, and the reproducible sedimentation difference in a subpopulation of Ste7 observed in the mutant, a much simpler explanation for the data is that increased dissociation of active Ste7 from the mutant scaffold is the primary cause of cross-talk. Our model also cannot directly explain the reduced steady-state phosphorylation of Ste7 in *ste5-E756G* cells. It is therefore possible, that the E756G mutation also reduces to some extent the ability of inactive Ste7 to bind the scaffold as well as the ability of active Ste7 to remain bound after being formed.

The findings here may be connected to previous observations that, like Ste5-E756G, kinase-defective mutants of Fus3 cause an increase in Kss1 phosphorylation in response to pheromone (Breitkreutz et al. 2001; Sabbagh et al. 2001). However, the mechanism by which Fus3 inhibits Kss1 phosphorylation is unknown. One possibility is that the recently reported phosphorylation of Ste5 by Fus3 may enhance the binding of the scaffold to Ste7 (Flotho et al. 2004).

Acknowledgements We thank Brad Cairns, Julie Brill, Gerry Fink, and Jeremy Thorner for antibodies, Sang-Hyun Park and Wendell Lim for advice on glycerol gradient centrifugation and anti-p42/44 blots, Lee Bardwell for protocols, Tomas Aragon and Peter Walter for advice on glycerol gradients and use of the Foxy Jr. fraction collector, Shivkumar Venkatasubrahmanyam for sequencing *ste5* alleles, Christine Guthrie, Anupama Seshan, Marc Meneghini, Marie Bao and Terry Shock provided critical comments on the manuscript. This work was supported by a grant from the National Institutes of Health (R01-GM63670–01).

References

Andersson J, Simpson DM, Qi M, Wang Y, Elion EA (2004) Differential input by Ste5 scaffold and Msg5 phosphatase route a MAPK cascade to multiple outcomes. EMBO J 23:2564–2576

Bao MZ, Schwartz MA, Cantin GT, Yates JR 3rd, Madhani HD (2004) Pheromone-dependent destruction of the Tec1 transcription factor is required for MAP kinase signaling specificity in yeast. Cell 119:991–1000

Bardwell L (2005) A walk-through of the yeast mating pheromone response pathway. Peptides 26:339–350

Bardwell L, Cook JG, Chang EC, Cairns BR, Thorner J (1996) Signaling in the yeast pheromone response pathway: specific and high-affinity interaction of the mitogen-activated protein (MAP) kinases Kss1 and Fus3 with the upstream MAP kinase kinase Ste7. Mol Cell Biol 16:3637–3650

Breitkreutz A, Boucher L, Tyers M (2001) MAPK specificity in the yeast pheromone response independent of transcriptional activation. Curr Biol 11:1266–1271

Bruckner S, Kohler T, Braus GH, Heise B, Bolte M, Mosch HU (2004) Differential regulation of Tec1 by Fus3 and Kss1 confers signaling specificity in yeast development. Curr Genet 46:331–342

Choi KY, Satterberg B, Lyons DM, Elion EA (1994) Ste5 tethers multiple protein kinases in the MAP kinase cascade required for mating in *S. cerevisiae*. Cell 78:499–512

Choi KY, Kranz JE, Mahanty SK, Park KS, Elion EA (1999) Characterization of Fus3 localization: active Fus3 localizes in complexes of varying size and specific activity. Mol Biol Cell 10:1553–1568

Chou S, Huang L, Liu H (2004) Fus3-regulated Tec1 degradation through SCFCdc4 determines MAPK signaling specificity during mating in yeast. Cell 119:981–990

van Drogen F, Stucke VM, Jorritsma G, Peter M (2001) MAP kinase dynamics in response to pheromones in budding yeast. Nat Cell Biol 3:1051–1059

Elion EA (2001) The Ste5p scaffold. J Cell Sci 114:3967–3978

Elion EA, Brill JA, Fink GR (1991) Functional redundancy in the yeast cell cycle: FUS3 and KSS1 have both overlapping and unique functions. Cold Spring Harb Symp Quant Biol 56:41–49

Errede B, Ge QY (1996) Feedback regulation of map kinase signal pathways. Philos Trans R Soc Lond B Biol Sci 351:143–148; discussion 148–149

Flatauer LJ, Zadeh SF, Bardwell L (2005) Mitogen-activated protein kinases with distinct requirements for Ste5 scaffolding influence signaling specificity in *Saccharomyces cerevisiae*. Mol Cell Biol 25:1793–1803

Flotho A, Simpson DM, Qi M, Elion EA (2004) Localized feedback phosphorylation of Ste5p scaffold by associated MAPK cascade. J Biol Chem 279:47391–47401

Golemis EA, Khazak V (1997) Alternative yeast two-hybrid systems. The interaction trap and interaction mating. Methods Mol Biol 63:197–218

Hall RA, Lefkowitz RJ (2002) Regulation of G protein-coupled receptor signaling by scaffold proteins. Circ Res 91:672–680

Harris K et al (2001) Role of scaffolds in MAP kinase pathway specificity revealed by custom design of pathway-dedicated signaling proteins. Curr Biol 11:1815–1824

Inagaki M, Schmelzle T, Yamaguchi K, Irie K, Hall MN, Matsumoto K (1999) PDK1 homologs activate the Pkc1-mitogen-activated protein kinase pathway in yeast. Mol Cell Biol 19:8344–8352

Inouye C, Dhillon N, Durfee T, Zambryski PC, Thorner J (1997) Mutational analysis of STE5 in the yeast *Saccharomyces cerevisiae*: application of a differential interaction trap assay for examining protein–protein interactions. Genetics 147:479–492

Madhani HD, Fink GR (1997) Combinatorial control required for the specificity of yeast MAPK signaling. Science 275:1314–1317

Madhani HD, Styles CA, Fink GR (1997) MAP kinases with distinct inhibitory functions impart signaling specificity during yeast differentiation. Cell 91:673–684

Mahanty SK, Wang Y, Farley FW, Elion EA (1999) Nuclear shuttling of yeast scaffold Ste5 is required for its recruitment to the plasma membrane and activation of the mating MAPK cascade. Cell 98:501–512

Maleri S, Ge Q, Hackett EA, Wang Y, Dohlman HG, Errede B (2004) Persistent activation by constitutive Ste7 promotes Kss1-mediated invasive growth but fails to support Fus3-dependent mating in yeast. Mol Cell Biol 24:9221–9238

Marcus S, Polverino A, Barr M, Wigler M (1994) Complexes between STE5 and components of the pheromone-responsive mitogen-activated protein kinase module. Proc Natl Acad Sci USA 91:7762–7766

McCaffrey G, Clay FJ, Kelsay K, Sprague GF Jr (1987) Identification and regulation of a gene required for cell fusion during mating of the yeast *Saccharomyces cerevisiae*. Mol Cell Biol 7:2680–2690

Morrison DK, Davis RJ (2003) Regulation of MAP kinase signaling modules by scaffold proteins in mammals. Annu Rev Cell Dev Biol 19:91–118

Park SH, Zarrinpar A, Lim WA (2003) Rewiring MAP kinase pathways using alternative scaffold assembly mechanisms. Science 299:1061–1064

Printen JA, Sprague GF Jr (1994) Protein–protein interactions in the yeast pheromone response pathway: Ste5p interacts with all members of the MAP kinase cascade. Genetics 138:609–619

Sabbagh W Jr, Flatauer LJ, Bardwell AJ, Bardwell L (2001) Specificity of MAP kinase signaling in yeast differentiation involves transient versus sustained MAPK activation. Mol Cell 8:683–691

Schwartz MA, Madhani HD (2004) Principles of MAP kinase signaling specificity in *Saccharomyces cerevisiae*. Annu Rev Genet 38:725–748

Sette C, Inouye CJ, Stroschein SL, Iaquinta PJ, Thorner J (2000) Mutational analysis suggests that activation of the yeast pheromone response mitogen-activated protein kinase pathway involves conformational changes in the Ste5 scaffold protein. Mol Biol Cell 11:4033–4049

Yablonski D, Marbach I, Levitzki A (1996) Dimerization of Ste5, a mitogen-activated protein kinase cascade scaffold protein, is required for signal transduction. Proc Natl Acad Sci USA 93:13864–13869

Yashar B et al (1995) Yeast MEK-dependent signal transduction: response thresholds and parameters affecting fidelity. Mol Cell Biol 15:6545–6553

Zhou Z, Gartner A, Cade R, Ammerer G, Errede B (1993) Pheromone-induced signal transduction in *Saccharomyces cerevisiae* requires the sequential function of three protein kinases. Mol Cell Biol 13:2069–2080